British Journal of Pharmacology

DOI:10.1111/j.1476-5381.2010.01081.x
www.brjpharmacol.org

RESEARCH PAPER

Negative cooperativity in binding of muscarinic receptor agonists and GDP as a measure of agonist efficacy

J Jakubík[1], H Janíčková[1], EE El-Fakahany[2] and V Doležal[1]

[1]*Institute of Physiology Academy of Sciences of the Czech Republic, Prague, Czech Republic, and* [2]*Division of Neuroscience Research in Psychiatry, University of Minnesota Medical School, Minneapolis, MN, USA*

Correspondence
Jan Jakubík, Institute of Physiology, AV ČR, v.v.i., Vídeňská 1083, 142 20 Praha, Czech Republic. E-mail: jakubik@biomed.cas.cz

Keywords
muscarinic acetylcholine receptors; agonist efficacy; GDP binding

Received
17 June 2010
Revised
23 August 2010
Accepted
22 September 2010

BACKGROUND AND PURPOSE

Conventional determination of agonist efficacy at G-protein coupled receptors is measured by stimulation of guanosine-5′-γ–thiotriphosphate (GTPγS) binding. We analysed the role of guanosine diphosphate (GDP) in the process of activation of the M_2 muscarinic acetylcholine receptor and provide evidence that negative cooperativity between agonist and GDP binding is an alternative measure of agonist efficacy.

EXPERIMENTAL APPROACH

Filtration and scintillation proximity assays measured equilibrium binding as well as binding kinetics of [^{35}S]GTPγS and [^{3}H]GDP to a mixture of G-proteins as well as individual classes of G-proteins upon binding of structurally different agonists to the M_2 muscarinic acetylcholine receptor.

KEY RESULTS

Agonists displayed biphasic competition curves with the antagonist [^{3}H]-N-methylscopolamine. GTPγS (1 μM) changed the competition curves to monophasic with low affinity and 50 μM GDP produced a similar effect. Depletion of membrane-bound GDP increased the proportion of agonist high-affinity sites. Carbachol accelerated the dissociation of [^{3}H]GDP from membranes. The inverse agonist N-methylscopolamine slowed GDP dissociation and GTPγS binding without changing affinity for GDP. Carbachol affected both GDP association with and dissociation from $G_{i/o}$ G-proteins but only its dissociation from $G_{s/olf}$ G-proteins.

CONCLUSIONS AND IMPLICATIONS

These findings suggest the existence of a low-affinity agonist-receptor conformation complexed with GDP-liganded G-protein. Also the negative cooperativity between GDP and agonist binding at the receptor/G-protein complex determines agonist efficacy. GDP binding reveals differences in action of agonists versus inverse agonists as well as differences in activation of $G_{i/o}$ versus $G_{s/olf}$ G-proteins that are not identified by conventional GTPγS binding.

Abbreviations

CHO cells, Chinese hamster ovary cells; GDP, guanosine diphosphate; GTPγS, guanosine-5′-γ–thiotriphosphate; NMS, N-methylscopolamine

Introduction

Almost 900 genes of the human genome encode several thousands of G-protein coupled receptors (GPCRs). GPCRs thus represent the largest family of receptors. The heterotrimeric guanine nucleotide-binding proteins (G-proteins) function to transduce signals from these receptors to effector systems including enzymes, such as adenylyl cyclase and phospholipase C and ion channels. Binding of an agonist to a GPCR induces conformational changes in the receptor protein that enable the receptor to promote guanosine diphosphate (GDP) release from the α-subunit of interacting heterotrimeric G-proteins (Gα) (Wess, 1997) and formation of a high-affinity complex with guanine nucleotide-free Gα (Kent *et al.*, 1980). The Gα subunit dissociates from the agonist-receptor-Gα complex upon binding of GTP and releases free Gα with bound GTP and βγ dimer, both of which are involved in regulation of the activity of various effector systems.

The biological activity of an agonist is a product of both affinity and efficacy. While affinity of an agonist for a receptor is strictly given by free binding energy, agonist efficacy in transducing a signal across the cell membrane depends on time-ordered complex conformational changes involving interactions among agonist, receptor, G-protein and guanine nucleotides. These interactions and the resulting conformational changes are less well characterized. In their pioneering work, De Lean *et al.* (1980) reported that GDP did not affect the efficacy of β-adrenoceptor agonists at G_s G-protein-coupled receptors. However, it has been repeatedly demonstrated that GDP affects binding of agonists at G_i G-protein coupled GPCRs (Florio and Sternweis, 1989; Tota and Schimerlik, 1990), muscarinic agonists decrease GDP binding (Haga *et al.*, 1986; Shiozaki and Haga, 1992) and accelerate its dissociation (Ferguson *et al.*, 1986). Although the structural basis for many steps in the G-protein nucleotide cycle have been clarified over the past decade, the precise mechanism for receptor-mediated G-protein activation (GDP-GTP exchange) remains incompletely defined largely because of difficulties in obtaining crystals of receptor G-protein complexes for X-ray diffraction analysis (Johnston and Siderovski, 2007; Oldham and Hamm, 2008).

The aim of our study was to investigate in detail the mechanisms that determine efficacy of agonists at individual classes of G-proteins coupled to M_2 muscarinic acetylcholine receptors in natural membrane environments. We performed detailed analyses of allosteric interactions between guanine nucleotides and four structurally distinct agonists exhibiting different potencies and efficacies at the M_2 receptor expressed in Chinese hamster ovary (CHO) cells. We showed that the efficacy of these agonists in stimulation of GTP binding correlates with the magnitude of negative cooperativity with GDP binding to the receptor G-protein complex. These data suggest that the decrease in GDP affinity due to acceleration of its dissociation plays a key role in determining agonist efficacy at the muscarinic M_2 receptor. We suggest that measurements of GDP binding provide additional information on receptor activation to that obtained from GTP binding assays. Most importantly, it reveals differences in the action of agonists and inverse agonists that are not observable in GTP binding studies.

Methods

Cell culture and membrane preparation

Chinese hamster ovary cells stably transfected with the human M_2 muscarinic receptor gene (CHO-M_2 cells) were kindly donated by Professor T.I.Bonner. Cell cultures and crude membranes were prepared as described previously (Jakubík *et al.*, 2006). Briefly, cells were grown to confluency in 75 cm^2 flasks in Dulbecco's modified Eagle's medium supplemented with 10% fetal bovine serum and 2×10^6 cells were subcultured to 100 mm Petri dishes. Medium was supplemented with 5 mM butyrate for the last 24 h of cultivation to increase receptor expression. Cells were detached by mild trypsinization on day 5 after subculture. Detached cells were washed twice in 50 mL of phosphate-buffered saline and 3 min centrifugation at 250× *g*. Washed cells were suspended in 20 mL of ice-cold incubation medium (100 mM NaCl, 20 mM Na-HEPES, 10 mM $MgCl_2$; pH = 7.4) supplemented with 10 mM EDTA and homogenized on ice by two 30 s strokes using Polytron homogenizer (Ultra-Turrax; Janke & Kunkel GmbH & Co. KG, IKA-Labortechnik, Staufen, Germany) with a 30 s pause between strokes. Cell homogenates were centrifuged for 30 min at 30 000× *g*. Supernatants were discarded, pellets resuspended in fresh incubation medium and centrifuged again. Resulting membrane pellets were kept at –20°C until assayed within a maximum of 10 weeks.

Preparation of GDP-less membranes

Membrane-bound GDP was removed by mild denaturation (Ferguson *et al.*, 1986). Membranes were incubated for 3 h in 1 M ammonium sulphate at 4°C, centrifuged and resuspended in incubation medium containing 20% glycerol for 1 h to allow renaturation. Then they were again centrifuged, resuspended in incubation medium, and used for experiments.

Equilibrium radioligand binding experiments

All radioligand binding experiments were optimized and carried out as described earlier (Jakubík *et al.*, 2006). Briefly, membranes were incubated in 96-well plates at 30°C in the incubation medium described above that was supplemented with freshly prepared dithiotreitol at a final concentration of 1 mM. Incubation volume was 200 µL or 800 µL for [^{3}H]N-methylscopolamine (NMS) saturation experiments. Approximately 30 and 10 µg of membrane proteins per sample were used for [^{3}H]NMS and [^{35}S]GTPγS binding respectively. NMS binding was measured directly in saturation experiments using six concentrations (30 pM to 1000 pM) of [^{3}H]NMS for 1 h. Depletion of radioligand was smaller than 20% for the lowest concentration. For calculations, radioligand concentrations were corrected for depletion. Agonist binding was determined in competition experiments with 1 nM [^{3}H]NMS. Membranes were first pre-incubated 60 min with agonists and guanine nucleotides, if applicable, and then incubated with [^{3}H]NMS for additional 120 min. Non-specific binding was determined in the presence of 10 µM NMS. Equilibrium [3H]GDP binding was measured after 5 h incubation. Non-specific binding was determined in the presence of 50 µM GDP. Agonist stimulated [^{35}S]GTPγS binding was measured in

a final volume of 200 μL of incubation medium with 500 pM of [^{35}S]GTPγS and 50 μM GDP for 20 min at 30°C after 60 min pre-incubation with GDP and agonist. Non-specific binding was determined in the presence of 1 μM unlabelled GTPγS. Incubations were terminated by filtration through Whatman GF/F glass fibre filters (Whatman, Maidstone, UK) using a Tomtech Mach III cell harvester (Perkin Elmer, Norwalk, CT, USA). Filters were dried in vacuum for 1 h at 80°C and then solid scintillator Meltilex A was melted on filters (105°C, 90 s) using a hot plate. The filters were cooled and counted in Wallac Microbeta scintillation counter.

Kinetic experiments

Kinetics of [^{35}S]GTPγS binding at GDP-less membranes was measured in a final volume of 200 μL at 30°C. Association of 1 nM [^{35}S]GTPγS with GDP-less membranes was measured after 20 min pre-incubation with buffer or carbachol ± 50 μM GDP. Dissociation of [^{35}S]GTPγS was initiated by 1 μM GTPγS alone or in mixture with carbachol after 90 min pre-incubation of GDP-less membranes with 1 nM [^{35}S]GTPγS ± 50 μM GDP. Kinetics of [^{3}H]GDP binding at $G_{i/o}$ and $G_{s/olf}$ G-proteins was measured using scintillation proximity assay (SPA) (DeLapp *et al.*, 1999) essentially as described earlier (Jakubík *et al.*, 2006). Association of 500 nM [^{3}H]GDP was measured after 20 min pre-incubation of GDP-less membranes with buffer or carbachol. Dissociation of [^{3}H]GDP was started by addition of 50 μM GDP alone or in mixture with carbachol after prelabelling GDP-less membranes with 500 nM [^{3}H]GDP for 180 min at 30°C. Dissociation was stopped by cooling and solubilization of samples by adding Nonidet P-40 to final concentration of 1% for 15 min. Primary polyclonal rabbit IgG antibody against α subunit of $G_{i/o}$ or $G_{s/olf}$ G-proteins in final dilution 1:1000 was then added and samples were incubated on ice for 60 min. Afterwards, 50 μL aliquots of anti-rabbit IgG coated scintillation beads were added (Amersham Bioscience, Buckinghamshire, UK; 500 mg of beads was resuspended in 40 mL of incubation buffer) and incubation continued for another 3 h. Trapped α subunits were pelleted at 4°C and 1500× *g* for 15 min and counted using SPA protocol in Wallac Microbeta scintillation counter.

Data analysis

In general binding data were analysed as described previously (Jakubík *et al.*, 2006). Data were preprocessed by Open Office 2.3 (http://www.openoffice.org) and subsequently analysed by Grace 5.1.18 (http://plasma-gate.weizman.ac.il/Grace) and statistic package R (http://www.r-project.org) on Mandriva distribution of Linux.

The following equations were fitted to data:

Saturation of radioligand binding

$$y = B_{MAX} \times x/(x + K_D) \qquad \text{(Eqn 1)}$$

y, binding of radioligand at free concentration of radioligand *x*; B_{MAX}, maximum binding capacity; K_D, equilibrium dissociation constant.

Concentration–response

$$y = 1 + (E_{MAX} - 1)/(1 + (EC_{50}/x)^{nH}) \qquad \text{(Eqn 2)}$$

y, radioactivity in the presence of agonist at concentration *x* normalized to radioactivity in the absence of agonist; E_{MAX}, maximal increase by agonist; EC_{50}, concentration of agonist producing 50% of maximal effect; nH, Hill coefficient.

Interference with [^{3}H]NMS or [^{3}H]GDP binding

$$y = 100 \times (1 - x^{nH}/(IC_{50} + x)^{nH}) \qquad \text{(Eqn 3)}$$

$$y = (100 - f_{low}) \times (1 - x/(IC_{50high} + x)) + f_{low} \times (1 - x/(IC_{50low} + x)) \qquad \text{(Eqn 4)}$$

y, binding of radioligand at a concentration of displacer *x* normalized to binding in the absence of displacer; IC_{50}, concentration causing 50% decrease in binding; nH, Hill coefficiet; f_{low}, percentage of low affinity sites; IC_{50high}, concentration causing 50% decrease in binding to high affinity sites; IC_{50low}, concentration causing 50% decrease in binding to low affinity sites. Both equations were fitted to data and the one giving better fit determined by *F*-test was used. Equilibrium dissociation constant of displacer (K_I) was calculated according to Cheng and Prusoff (Cheng and Prusoff, 1973).

Rate of association

$$y = B_{eq} \times [1 - \exp(-1 \times k_{obs} \times x)] \qquad \text{(Eqn 5a)}$$

$$y = B_{eq1} \times (1 - \exp(-1 \times k_{obs1} \times x)) + B_{eq2} \times [1 - \exp(-1 \times k_{obs2} \times x)] \qquad \text{(Eqn 5b)}$$

y, binding of radioligand at time *x*; k_{obs}, k_{obs1}, k_{obs2}, observed rates of association; B_{eq}, B_{eq1}, B_{eq2}, equilibrium binding.

Rate of radioligand dissociation

$$y = 100 \times e^{(-koff \times x)} \qquad \text{(Eqn 6a)}$$

$$y = (100 - f_2) \times e^{(-koff1 \times x)} + f_2 \times e^{(-koff2 \times x)} \qquad \text{(Eqn 6b)}$$

y, binding of radioligand at time *x* normalized to time 0; k_{off}, k_{off1}, k_{off2}, rate constants; f_2, percentage of sites with rate constant k_{off2}.

Allosteric interaction of radioligand

Allosteric interaction between a radioligand and an allosteric modulator was analysed according to the ternary complex model (Ehlert, 1988).

$$y = \frac{[D] + K_D}{[D] + \dfrac{K_D \times (K_A + x)}{K_A + x/\alpha}} \qquad \text{(Eqn 7)}$$

y, binding of radioligand in the presence of ligand A at concentration *x* normalized to the absence of ligand A; [D] concentration of radioligand; K_D, equilibrium dissociation constant of radioligand; K_A; equilibrium dissociation constant of ligand A; α, factor of cooperativity between radioligand and ligand A.

Allosteric interaction between GDP and agonist binding

Allosteric interaction between GDP and agonist binding was analysed according to the ternary complex model with agonists competing with radioligand (Jakubík *et al.*, 1997).

$$y = \frac{[D] + K_D}{[D] + \frac{K_D \times ([A] \times (K_A + x/\beta) + K_I \times (K_A + x))}{K_I \times (K_A + x/\alpha)}} \quad \text{(Eqn 8)}$$

y, binding of radioligand ([^{3}H]NMS) in the presence of GDP at concentration x normalized to the absence of GDP; [D] concentration of radioligand; K_D, equilibrium dissociation constant of radioligand; [A], concentration of agonist; K_I, equilibrium dissociation constant of high affinity agonist binding form Eqn 3; K_A, equilibrium dissociation constant of allosteric ligand (GDP); α, factor of cooperativity between radioligand and allosteric ligand from Eqn 7 (always 1); β, factor of cooperativity between allosteric ligand and agonist.

Materials

The radioligands [^{3}H]NMS ([^{3}H]GDP), [^{35}S]GTPγS and anti-rabbit IgG-coated scintillation proximity beads were from Amersham (UK). Rabbit polyclonal antibodies against C-terminus of G-protein ($G_{i/o}$, C-10, and $G_{s/olf}$, C-18) were from Santa Cruz Biotechnology (Santa Cruz, CA, USA) Carbachol, dithiotreitol, EDTA, GDP, GTPγS, NMS chloride and pilocarpine were from Sigma (St. Louis, MO, USA). Oxotremorine was from RBI (Natick, MA, USA) and Nonidet P-40 was from USB Corporation (Cleveland, OH, USA). Furmethide was kindly donated by Dr Shelkovnikov (University of St. Petersburg, Russia). Nomenclature of receptors and G-proteins follows Alexander *et al*. (2009).

Results

General characterization of crude membranes

Experiments were performed on membranes of CHO-M_2 cells stably expressing 1.4 ± 0.2 pmol of binding sites for [^{3}H]NMS chloride per mg of membrane protein. The equilibrium dissociation constant (K_D) of [^{3}H]NMS was 512 ± 32 pM (mean ± SEM, n = 4, measurements on cells from independent seedings). Total binding of [^{35}S]GTPγS to crude membranes was 123 ± 18 pmol per mg of protein out of which 74 ± 11 pmol was to $G_{i/o}$, 21 ± 3 pmol to $G_{q/11}$ and 16 ± 3 pmol to $G_{s/olf}$ G-proteins respectively (means ± SEM, n = 3).

Carbachol, furmethide, oxotremorine and pilocarpine concentration dependently stimulated binding of [^{35}S]GTPγS (Figure 1, Table 1). Carbachol and furmethide induced similar maximal increase of [^{35}S]GTPγS binding (threefold and 3.1-fold increase respectively) with half-effective concentrations (EC_{50}) of 12.3 and 7.0 µM respectively. Oxotremorine and pilocarpine were more potent (EC_{50} = 1.0 and 1.2 µM respectively) but less efficacious (E_{max} = 2.8 and 1.6-fold increase respectively). The rank order of efficacy was: furmethide = carbachol > oxotremorine > pilocarpine, with a ranking of potency of: oxotremorine = pilocarpine > furmethide = carbachol. Carbachol had no effect on [^{35}S]GTPγS binding at wild-type (non-transfected) CHO cells.

Influence of guanine nucleotides on the affinity of agonists

Affinity of agonist binding was assessed indirectly in competition experiments with 1 nM of the muscarinic radioligand [^{3}H]NMS (Figure 2). Competition curves were biphasic and

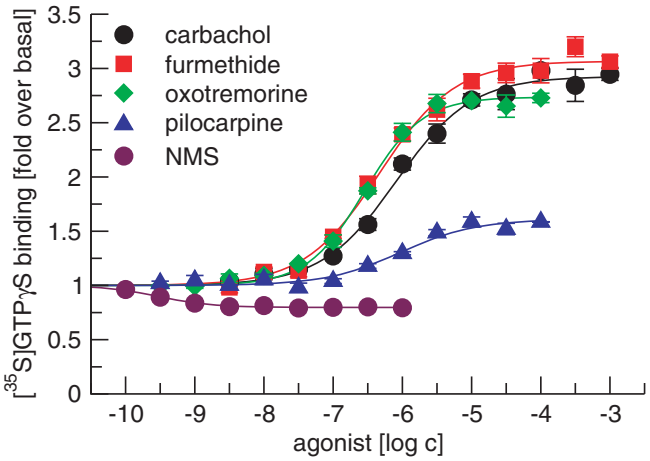

Figure 1

Stimulation of [^{35}S]guanosine-5′-γ–thiotriphosphate (GTPγS) binding by agonists. [^{35}S]GTPγS binding to membranes stimulated by increasing concentrations (abscissa, log M) of agonists carbachol, furmethide, oxotremorine, pilocarpine and antagonist N-methylscopolamine (NMS) is expressed as fold over basal (ordinate). Data are mean ± SEM of values from three experiments performed in quadruplicate. Curves were fitted using Equation 2 and results of fits are shown in the Table 1.

displayed a similar proportion (50 to 66%) of low-affinity binding sites for all agonists but different affinities for both high- and low-affinity binding sites (Table 2). High-affinity binding ranged from 12 nM for oxotremorine to 120 nM for carbachol and low-affinity binding from 580 nM for oxotremorine to 9 µM for carbachol. Competition curves between [^{3}H]NMS and agonists in the presence of 1 µM GTPγS expectedly became monophasic for all agonists (Figure 2) with calculated equilibrium inhibition constants (K_I) corresponding to the low-affinity K_I in the absence of GTPγS. Similarly, 50 µM GDP present during competition measurements (Figure 2) also converted curves to monophasic ones with K_I corresponding to that in the presence of GTPγS and the low-affinity K_I in the absence of added nucleotides (Figure 2, Table 2).

In order to explore the effects of added GDP on agonist binding, we reduced membrane-bound native GDP by inducing its dissociation under slightly denaturing conditions, washing and renaturing as described in *Methods*. Competition curves remained biphasic (Figure 2) but the proportion of low-affinity sites decreased fivefold to sevenfold compared with membranes before treatment (Table 2). Low-affinity K_I of agonists corresponded to the low-affinity K_I under control conditions. High-affinity K_I values were significantly lower for carbachol and oxotremorine (twofold and fourfold respectively) and not changed for oxotremorine and pilocarpine.

Characterization of GDP-depleted membranes

In comparison with crude membranes, depletion of GDP did not change the affinity for [^{3}H]NMS (498 ± 29 pM) but increased the number of binding sites per mg of protein to 24 ± 3 pmol (mean ± SEM, n = 4). On the other hand, total binding of [^{35}S]GTPγS per mg of protein fell to 28 ± 2 pmol

Table 1

Parameters of agonist-stimulated [^{35}S]GTPγS binding to membranes from M_2 CHO cells

	pEC_{50}	E_{MAX} [fold over basal]	nH
Carbachol	4.91 ± 0.04*	3.01 ± 0.07	0.81 ± 0.05
Furmethide	5.15 ± 0.05	3.12 ± 0.08	0.82 ± 0.05
Oxotremorine	5.99 ± 0.04**	2.78 ± 0.06*	0.92 ± 0.03
Pilocarpine	5.93 ± 0.08**	1.59 ± 0.06***	0.98 ± 0.03

Constants and Hill coefficients (nH) were obtained by fitting Equation 2 to data from individual experiments shown in Figure 1. Half-effective molar concentration of agonists is expressed as negative logarithm (pEC_{50}) and maximal stimulation (E_{MAX}) as fold increase over basal binding. Data are means ± SEM of values from three individual experiments performed in quadruplicates. *P < 0.05, significantly different from furmethide; **P < 0.01, significantly different from carbachol and furmethide; ***P < 0.001, significantly different from all other agonists by ANOVA and Tukey's test.
CHO cells, Chinese hamster ovary cells; GTPγS, guanosine-5′-γ–thiotriphosphate.

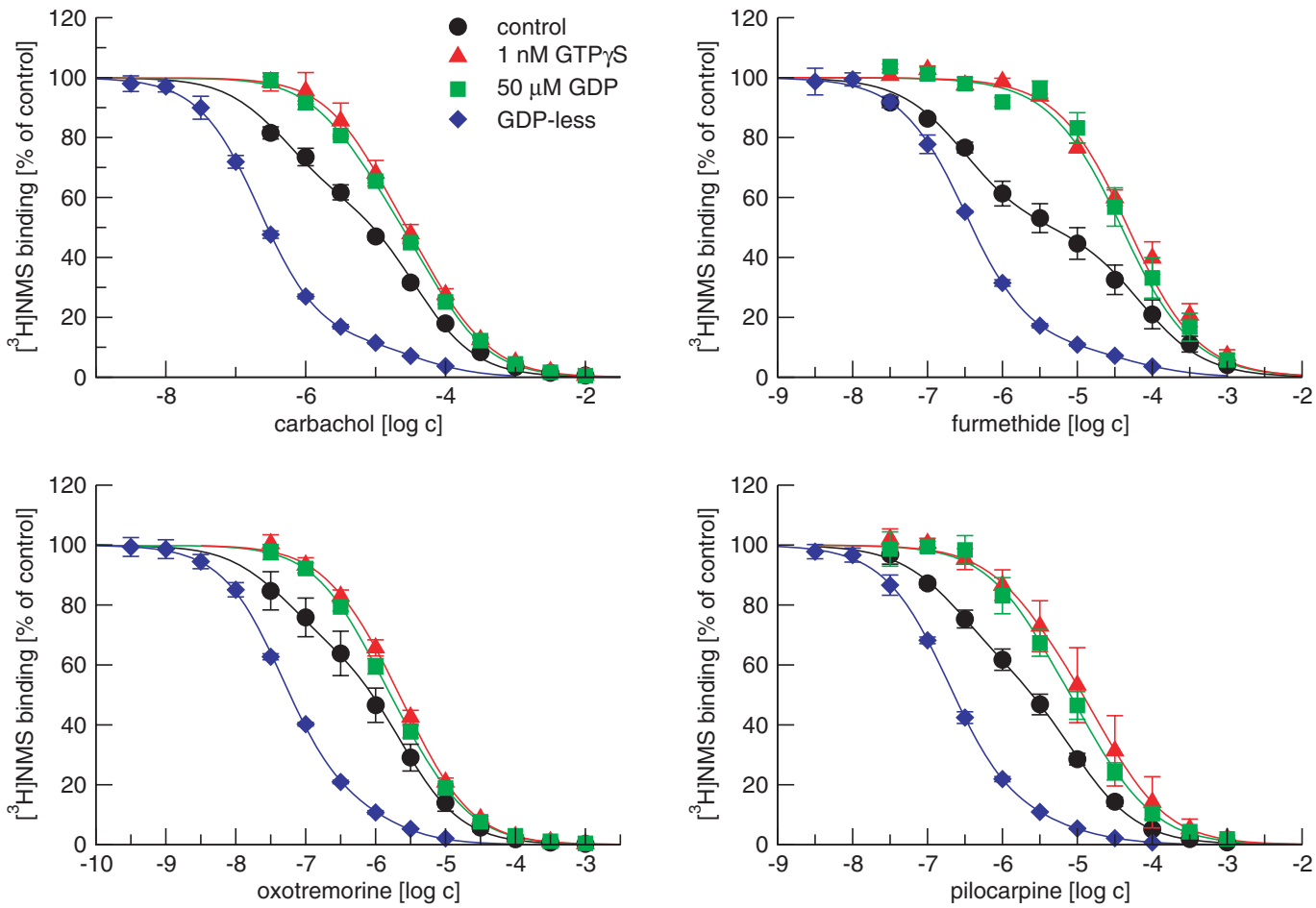

Figure 2

Effects of guanine nucleotides on competition between agonists and [^{3}H]N-methylscopolamine (NMS) binding. Binding of 1 nM [^{3}H]NMS to membranes in the presence of increasing concentrations (abscissa, log M) of the agonists carbachol (upper left), furmethide (upper right), oxotremorine (lower left) and pilocarpine (lower right) is expressed as per cent of control binding in the absence of agonist. Data are shown for binding to crude membranes (control); binding to crude membranes in the presence of 50 μM guanosine diphosphate (GDP); binding to crude membranes in the presence of 1 μM guanosine-5′-γ–thiotriphosphate (GTPγS); and binding to GDP-less membranes. Data are mean ± SEM of values from three experiments performed in quadruplicate. Curves were fitted using Equations 3 and 4. Results of fits are shown in the Table 2.

Table 2

Effects of guanine nucleotides on binding parameters of muscarinic agonists

		Carbachol	Furmethide	Oxotremorine	Pilocarpine
Control	$pK_{i\ high}$	6.92 ± 0.08	7.12 ± 0.09	7.93 ± 0.07	7.19 ± 0.08
	$pK_{i\ low}$	5.04 ± 0.08	4.78 ± 0.08	6.24 ± 0.07	5.65 ± 0.08
	f_{low} [%]	59 ± 11	50 ± 9	66 ± 8	58 ± 9
+1 μM GTPγS	pK_i	5.13 ± 0.05	4.76 ± 0.05	6.26 ± 0.04	5.54 ± 0.06
+50 μM GDP	pK_i	5.19 ± 0.06	4.77 ± 0.05	6.38 ± 0.04	5.67 ± 0.05
GDP-less membranes	$pK_{i\ high}$	7.27 ± 0.08*	7.77 ± 0.08**	7.95 ± 0.07	7.33 ± 0.07
	$pK_{i\ low}$	4.99 ± 0.09	4.87 ± 0.09	6.49 ± 0.08	5.69 ± 0.10
	f_{low} [%]	12 ± 4**	9.6 ± 3.8**	13 ± 4**	7.9 ± 3.2**

Equilibrium inhibition constants K_I and percentages of low affinity sites were obtained by fitting Equations 3 and 4 to data from individual experiments shown in Figure 2. K_I values of agonists are expressed as negative logarithms of molar concentration (pK_i). f_{low} is the fraction of receptors in the low-affinity state. Data are means ± SEM of values from three independent experiments performed in quadruplicates. *P < 0.05; **P < 0.01, significantly different from corresponding control membranes by t-test.
GDP, guanosine diphosphate.

Table 3

Rate constants of [^{35}S]GTP-γS binding in GDP-less membranes

	k_{obs} [h^{-1}]	B_{eq} [fmol·μg^{-1} protein]	k_{off} [h^{-1}]
GDP-less membranes	4.35 ± 0.15	5.66 ± 0.22	0.324 ± 0.013
+100 μM carbachol	4.33 ± 0.17	5.70 ± 0.25	0.327 ± 0.014
50 μM GDP	1.34 ± 0.14*	1.21 ± 0.12*	0.334 ± 0.012
+100 μM carbachol	3.98 ± 0.14*[a]	4.85 ± 0.19*[a]	0.322 ± 0.012
+100 nM NMS	1.01 ± 0.08[a]	1.20 ± 0.11	0.343 ± 0.009

Constants were obtained by fitting Equations 5a or 6a as appropriate to data from individual experiments shown in Figure 3. k_{obs}, association rate constant; B_{eq}, binding at equilibrium; k_{off}, dissociation rate constant. Data are means ± SEM of values from three independent experiments performed in quadruplicates.*P < 0.01; significantly different from control (GDP vs. GDP-less, with vs. without carbachol) and [a]P < 0.05; significantly different from control without ligand by t-test.
GDP, guanosine diphosphate; GTPγS, guanosine-5′-γ–thiotriphosphate; NMS, N-methylscopolamine.

out of which 18 ± 1 pmol was to $G_{i/o}$, 3.5 ± 0.5 pmol to $G_{q/11}$ and 4.6 ± 0.6 pmol to $G_{s/olf}$ G-proteins respectively (means ± SEM, n = 3).

Kinetics of [^{35}S]GTPγS binding to membranes

Measurements of 1 nM [^{35}S]GTPγS binding kinetics were carried out on GDP-depleted membranes without (Figure 3, left) or with added 50 μM GDP (Figure 3, right). As shown in Table 3, addition of GDP slowed down the rate of association 3.2-fold, decreased equilibrium binding 4.7-fold, but did not change the rate of dissociation (Figure 3, Table 3). A saturating concentration of carbachol (100 μM) did not change kinetics of [^{35}S]GTPγS binding in the absence of GDP (Figure 3, left, open circles). In the presence of GDP, carbachol had no effect on the rate of dissociation of [^{35}S]GTPγS but accelerated the rate of association 2.6-fold and increased equilibrium binding fourfold (to 92 and 90% of that in the absence of GDP respectively). In the presence of GDP, the inverse agonist NMS slowed the association of [^{35}S]GTPγS by 25% and, similarly to carbachol, did not change dissociation kinetics (Table 3).

Kinetics of [^{3}H]GDP binding to membranes

Measurements of 500 nM [^{3}H]GDP binding kinetics (Figure 4) were carried out on GDP-less membranes in the absence or in the presence of 10 μM or 100 μM carbachol or 0.1 μM NMS. Association of [^{3}H]GDP was biphasic with an observed association rate ($k_{obs\ slow}$) of 0.010 min^{-1} for 44% of sites and $k_{obs\ fast}$ of 0.063 min^{-1} for the rest. Ten μM carbachol decelerated association of the slower fraction sevenfold while it slowed down that at the faster fraction by only twofold. Carbachol (100 μM) brought further slowing down of both the slower and faster fractions to 0.00024 min^{-1} and 0.013 min^{-1} respectively. Dissociation of [^{3}H]GDP was also biphasic with dissociation rate constants $k_{off\ slow}$ 0.85 min^{-1} for 40% of sites and $k_{off\ fast}$ 0.073 min^{-1} for the rest. Carbachol accelerated [^{3}H]GDP dissociation from the faster fraction more than 100-fold at both concentrations while the rate at the slower fraction was

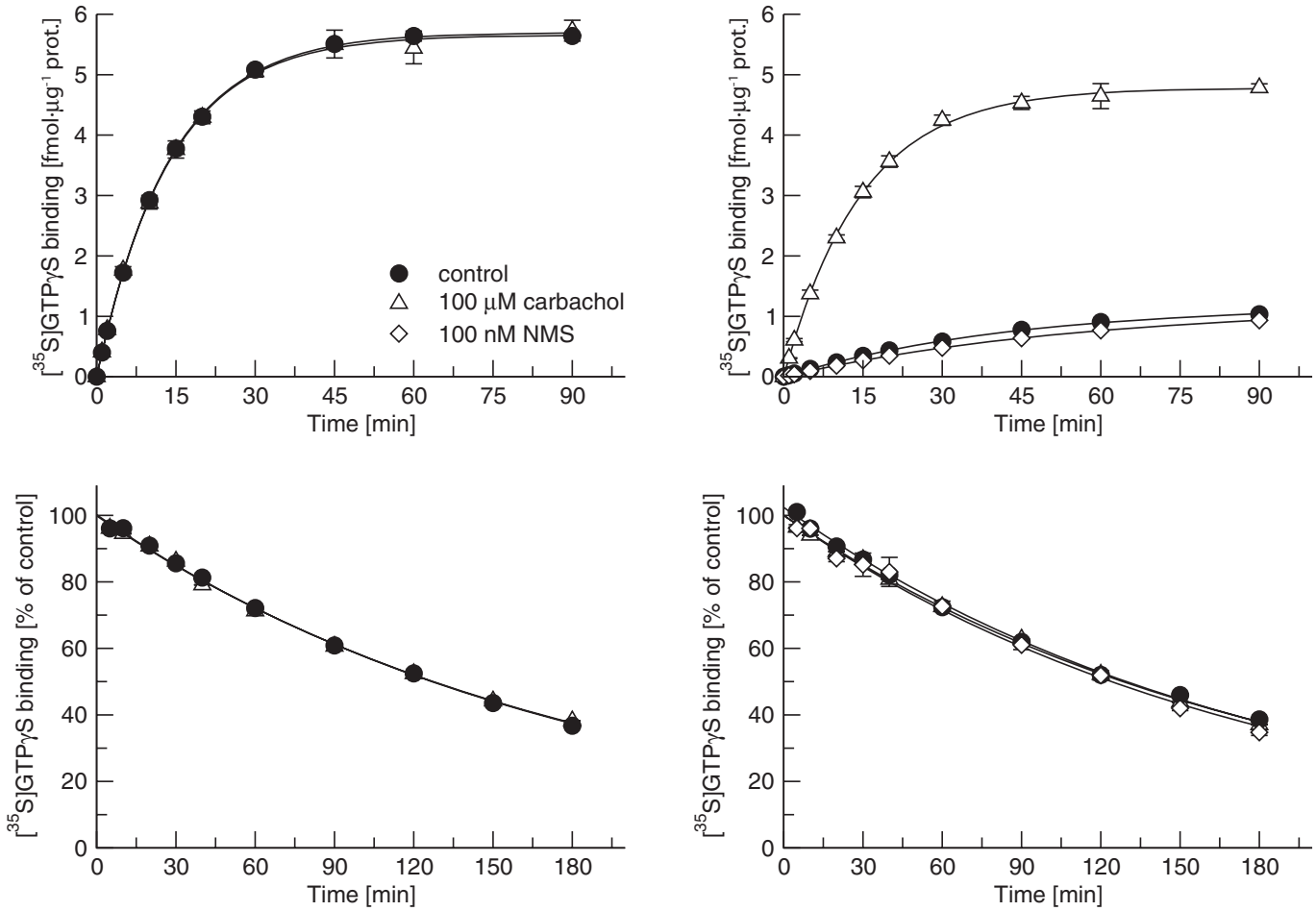

Figure 3

Kinetics of [^{35}S]guanosine-5′-γ–thiotriphosphate (GTPγS) binding to membranes. Time course of association of 1 nM [^{35}S]GTPγS with (top row) and dissociation from (bottom row) GDP-less membranes. Binding was carried out either in the absence (left graphs) or presence (right graphs) of 50 µM GDP in the absence or presence of 100 µM carbachol or 100 nM N-methylscopolamine (NMS). Data are presented as mean ± SEM of values from three experiments performed in quadruplicate. Curves were fitted using Equations 5 (association) or 6 (dissociation). Results of fits are shown in the Table 3.

reduced threefold and fourfold at 10 and 100 µM carbachol, respectively.

Allosteric interactions between GDP and agonists

Carbachol-induced changes in GDP kinetics confirmed allosteric interactions between GDP and carbachol. In order to quantify allosteric interactions between GDP and agonists, their affinities to free receptor-G-protein complex had to be known. Affinity of GDP was determined in equilibrium binding of [^{3}H]GDP to GDP-less membranes in homologous competition (Figure 5 left) and saturation (Figure 5 right) experiments. Homologous competition curves of 1 µM and 5 µM [^{3}H]GDP were monophasic with Hill coefficient equal to 1 and IC_{50} values 4.48 (95% interval of confidence 3.93–5.02) and 8.55 (95% interval of confidence 7.62–9.59) µM, respectively, giving K_D for [^{3}H]GDP of 3.49 µM. In accordance with competition experiments, saturation binding of GDP-less membranes with 0.3 to 10 µM [^{3}H]GDP displayed K_D of 3.47 ± 0.03 µM and B_{MAX} of 28 ± 3 fmol of binding sites per µg of protein.

In the first set of experiments to quantify the magnitude of allosteric interactions between GDP and agonists, the binding of [^{3}H]GDP at fixed 10 µM concentration and increasing concentrations of tested agonists was measured in competition-like experiments (Figure 6). While the inverse agonist NMS did not affect [^{3}H]GDP binding, all the tested agonists decreased it. Fitting Eqn 7 to data using all four agonists gave the same equilibrium dissociation constant for [^{3}H]GDP (pK_A 5.51 ± 0.05; mean ± SD; n = 12). Factors of cooperativity α between binding of [^{3}H]GDP and carbachol, furmethide, oxotremorine and pilocarpine were (expressed as pα) –2.3 ± 0.2, –2.4 ± 0.3, –1.8 ± 0.1 and –1.4 ± 0.1 (mean ± SEM., n = 3) respectively.

In the second set of experiments determining the magnitude of allosteric interactions between GDP and agonists, we employed [^{3}H]NMS as a tracer because of the high cost of [^{3}H]GDP and difficulties in quantifying negative cooperativity

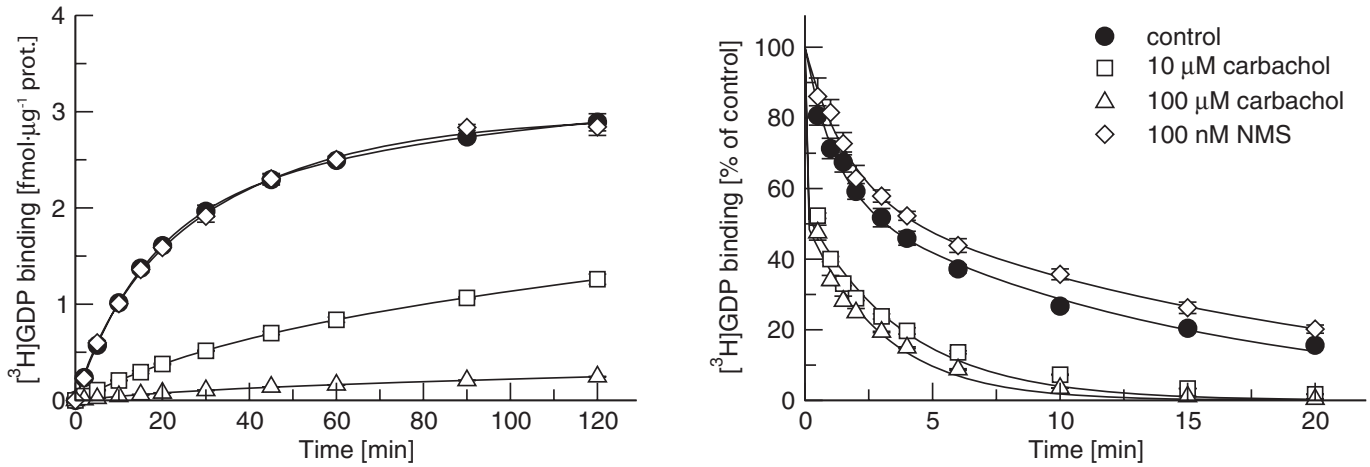

Figure 4

Kinetics of [^{3}H]GDP binding to membranes. Time course of association 500 nM [^{3}H]GDP with (left) and dissociation from (right) GDP-less membranes in the absence or presence of 10 µM or 100 µM carbachol or 100 nM N-methylscopolamine (NMS). Data are expressed as mean ± SEM of values from three experiments performed in quadruplicate. Curves were fitted using Equations 5 (association) or 6 (dissociation).

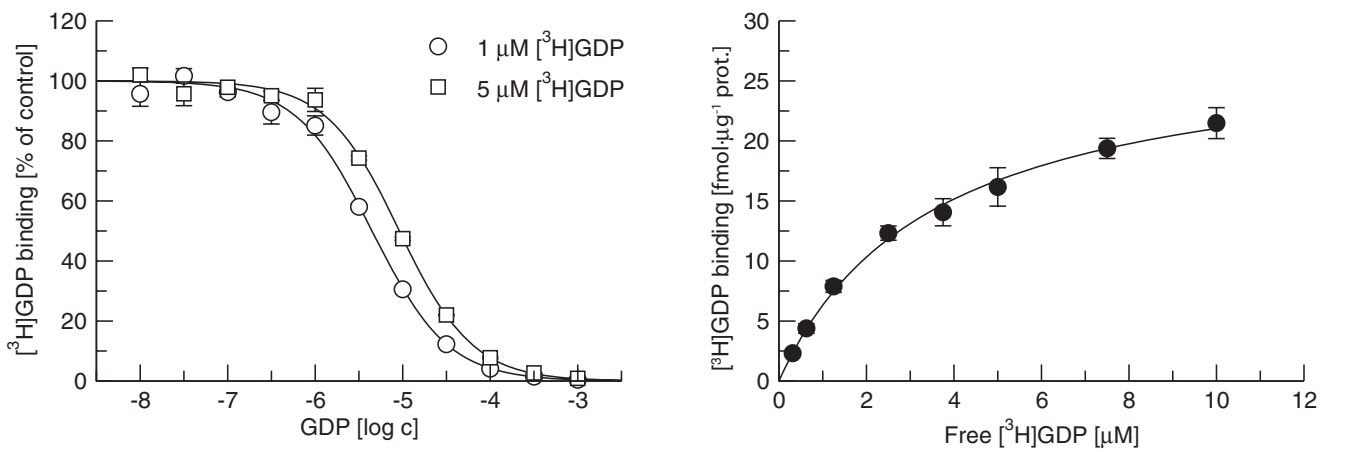

Figure 5

Equilibrium binding of [^{3}H]GDP to membranes. Left: Homologous competition of GDP (abscissa, log M concentration of GDP) with 1 µM and 5 µM [^{3}H]GDP binding (ordinate, percent of control binding). Right: [^{3}H]GDP saturation binding (abscissa, concentration in µM; ordinate, [^{3}H]GDP binding in fmol·µg^{-1} protein). Data are presented as mean ± SEM of values from three experiments performed in quadruplicate. Curves were fitted using Equations 1 and 3 as appropriate.

between GDP and full agonist (carbachol, furmethide) binding. The magnitude of negative cooperativity between agonists and GDP in these experiments was derived from a decrease in displacement of [^{3}H]NMS binding by a fixed concentration of tested agonist by increasing concentrations of GDP in GDP-less membranes. In the absence of agonist, GDP had no effect on [^{3}H]NMS binding (Figure 7). Eqn 7 could not be fitted to the data and the factor of cooperativity α between [^{3}H]NMS and GDP is thus equal to 1. Agonists competed with [^{3}H]NMS and diminished its binding (Figure 7). GDP allosterically reduced the affinity for agonists that was manifested as an increase in [^{3}H]NMS binding. Factors of cooperativity β between GDP and agonists were calculated by fitting Eqn 8 to the data shown in Figure 7. GDP diminished the affinity of the full agonists furmethide and carbachol 250-fold and 200-fold, respectively, while the affinity of the partial agonists oxotremorine and pilocarpine was reduced only 60-fold and 25-fold respectively. Estimated affinity for GDP was 3.2 µM (pK_A = –5.49 ± 0.03; mean ± SEM.; n = 12) for all fits.

Agonist stimulation of [^{35}S]GTPγS binding to individual G-proteins

Binding of [^{35}S]GTPγS to individual subclasses of G-proteins was measured in SPAs (Figure 8). As expected, all tested agonists stimulated binding of [^{35}S]GTPγS to Gi/o G-proteins with higher potency than to $G_{s/olf}$ and $G_{q/11}$ G-proteins (Table 4). The rank order of potencies was oxotremorine = pilocarpine > furmethide > carbachol at all tested G-protein subclasses

(except no stimulation of [^{35}S]GTPγS binding by oxotremorine at $G_{q/11}$ was detected). Agonists were also more efficacious in stimulating [^{35}S]GTPγS binding at $G_{i/o}$ G-proteins than at the other two G-protein classes. The rank order of agonist efficacies to stimulate [^{35}S]GTPγS binding varied among G-protein classes and was as follows: furmethide = carbachol = oxotremorine > pilocarpine at $G_{i/o}$, carbachol = furmethide > oxotremorine > pilocarpine at $G_{s/olf}$, and carbachol > furmethide > pilocarpine > oxotremorine at $G_{q/11}$.

Kinetics of [^{3}H]GDP binding to individual subclasses of G-proteins

Kinetics of 500 nM [^{3}H]GDP binding at individual subclasses of G-proteins measured in SPA is shown in Figure 9.

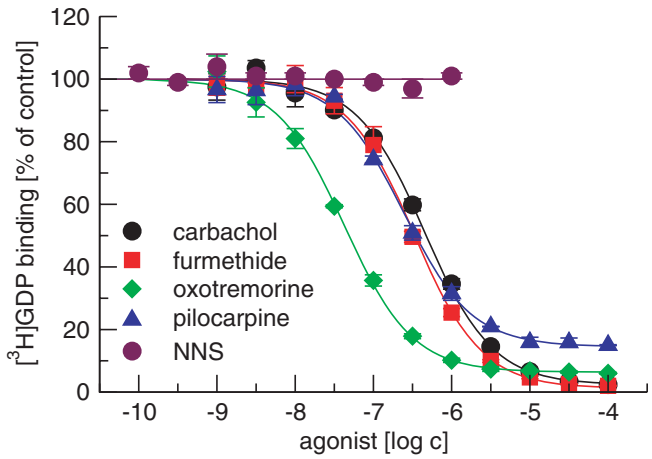

Figure 6

Direct measurement of allosteric interactions between agonists and [^{3}H]GDP at membranes. The magnitude of allosteric interactions between agonists (carbachol, furmethide, oxotremorine, pilocarpine) or antagonist [N-methylscopolamine (NMS)] and GDP was measured directly as changes in equilibrium binding of 10 μM [^{3}H]GDP to GDP-less membranes in the presence of increasing ligand concentration (abscissa, log M). Data are expressed as mean ± SEM of values from three experiments performed in quadruplicate. Curves were fitted using Equation 7.

Association of [^{3}H]GDP with the $G_{i/o}$ subclass of G-proteins that preferentially couple with the M_2 receptors was biphasic (Figure 9, top left) with twice as many sites with fast (k_{obs1} = 0.055 min^{-1}) as with slow (k_{obs} = 0.011 min^{-1}) association kinetics (Table 5). Carbachol converted the association curve to become monophasic and decreased equilibrium binding 1.8-fold and ninefold at 10 and 100 μM concentrations respectively. Carbachol (100 μM) slowed down the association of [^{3}H]GDP 12-fold in comparison to fast sites or 10-fold in comparison to mono-exponential fit of association data under control conditions (in the absence of carbachol) (k_{obs} = 0.042 ± 0.005 min^{-1}; B_{eq} = 2.8 ± 0.3 fmol·μg·prot^{-1}; mean ± SEM; n = 3). Dissociation curves were biphasic in the absence as well as in the presence of carbachol with 36 to 38% of slow binding sites. Carbachol accelerated the dissociation rate to a similar extent from both slow and fast sites. Acceleration was 6.3–6.5-fold by 10 μM carbachol and eightfold by 100 μM carbachol respectively (Figure 9, lower left; Table 5).

Muscarinic M_2 receptors also couple non-preferentially with the $G_{s/olf}$ and $G_{q/11}$ subclasses of G-proteins. We therefore attempted to determine the influence of carbachol on the kinetics of [^{3}H]GDP binding at these two other major G-protein subclasses. Unlike the results obtained for the $G_{i/o}$ subclass, association and dissociation curves of [^{3}H]GDP binding with $G_{s/olf}$ were monophasic in the absence as well as in the presence of carbachol (Figure 9, right column). Carbachol had no effect on [^{3}H]GDP binding association rate, accelerated [^{3}H]GDP dissociation rate 1.8-fold and threefold, and decreased equilibrium binding 1.9-fold and 8.1-fold at 10 and 100 μM carbachol respectively (Figure 9, top right, Table 5). We were not able to determine the kinetics of [^{3}H]GDP binding at $G_{q/11}$ subclass of G-proteins due to extremely fast on and off rates.

Allosteric interactions between GDP and agonists at individual subclasses of G-proteins

Effects of agonists on equilibrium binding of 10 μM [^{3}H]GDP to individual subclasses of G-proteins was measured in SPA (Figure 10, Table 6). All agonists decreased [^{3}H]GDP binding to $G_{i/o}$ (Figure 10, upper left) and $G_{s/olf}$ (Figure 10, upper right)

Table 4

Parameters of [^{35}S]GTPγS binding to $G_{i/o}$, $G_{s/olf}$ and $G_{q/11}$ subtypes of G-proteins

	$G_{i/o}$ pEC_{50}	E_{MAX}	$G_{s/olf}$ pEC_{50}	E_{MAX}	$G_{q/11}$ pEC_{50}	E_{MAX}
carbachol	5.11 ± 0.06	2.89 ± 0.06	4.25 ± 0.06	1.82 ± 0.05	4.37 ± 0.02	1.61 ± 0.02
furmethide	5.34 ± 0.10	2.95 ± 0.09	4.76 ± 0.03*	1.70 ± 0.02	4.72 ± 0.06*	1.20 ± 0.01*
oxotremorine	6.03 ± 0.05**	2.72 ± 0.05	5.13 ± 0.04**	1.53 ± 0.01**	n.c.	n.c.***
pilocarpine	5.95 ± 0.06**	1.52 ± 0.05***	5.05 ± 0.05**	1.10 ± 0.01***	4.95 ± 0.05**	1.08 ± 0.01***

Constants and Hill coefficients (nH) were obtained by fitting Equation 2 to data from individual experiments shown in Figure 1. Half effective molar concentration of agonists is expressed as negative logarithm (pEC_{50}) and maximal stimulation (E_{MAX}) as fold increase over basal binding. Data are means ± SEM of values from three individual experiments performed in quadruplicates. *P < 0.05, significantly different from carbachol; **P < 0.01, significantly different from carbachol and furmethide; ***P < 0.001, significantly different from all other agonists by ANOVA and Tukey's test.

GTPγS, guanosine-5′-γ–thiotriphosphate; n.c., no convergence.

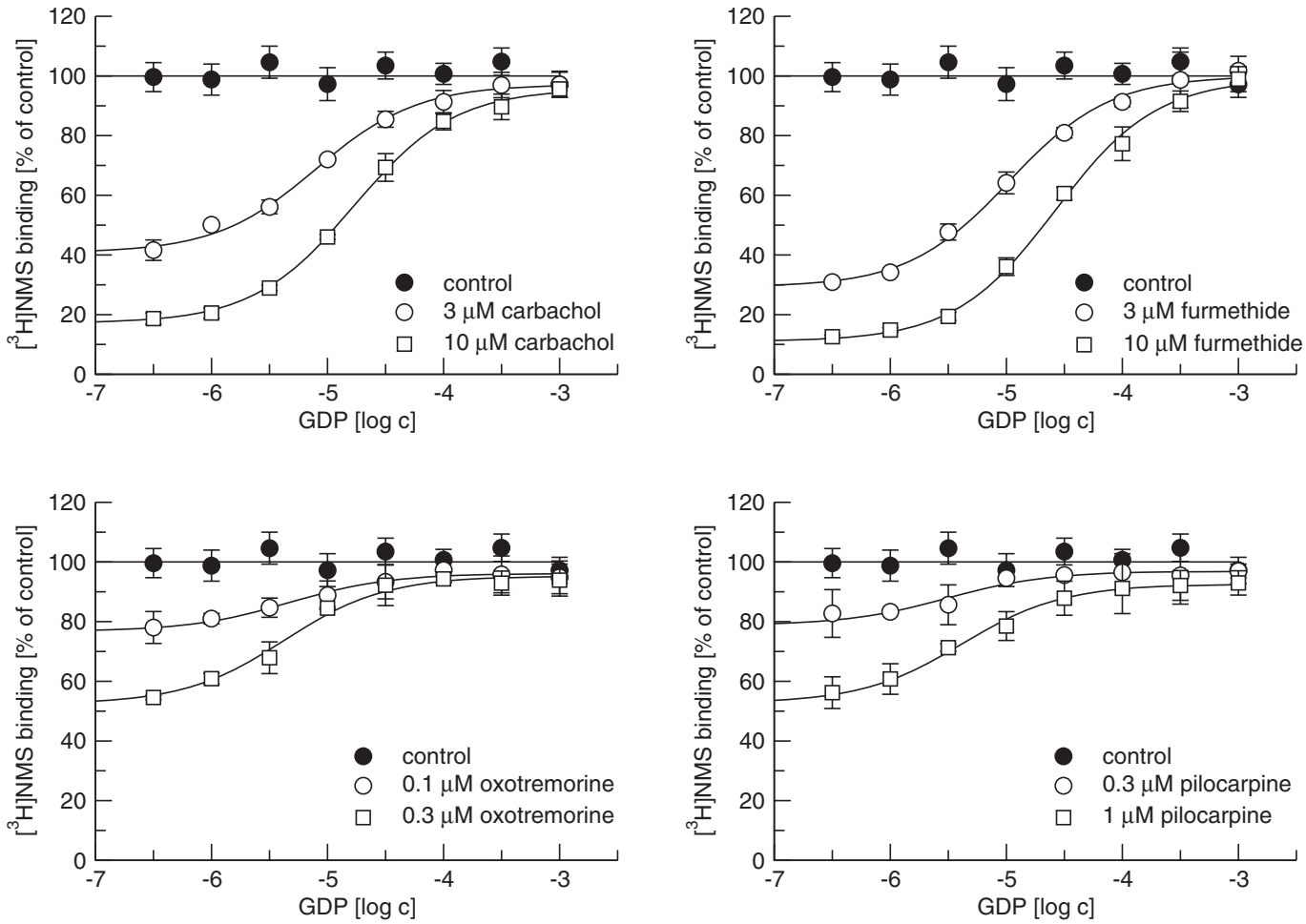

Figure 7

Indirect measurement of allosteric interactions between agonists and GDP at membranes. The magnitude of allosteric interactions between agonists (carbachol, upper left; furmethide, upper right; oxotremorine, lower left; pilocarpine, lower right) and GDP was measured indirectly as changes in equilibrium binding of 1 nM [^{3}H]N-methylscopolamine (NMS) to GDP-less membranes in the presence of a fixed concentration of agonist and increasing concentrations of GDP (abscissa, log M). Binding of 1 nM [^{3}H]NMS in the absence of agonis is also shown (control). Carbachol and furmethide were used at 3 and 10 μM, oxotremorine at 0.1 and 0.3 μM, and pilocarpine at 0.3 and 1 μM. Data are presented as mean ± SEM of values from three experiments performed in quadruplicate. Curves were fitted using Equations 7 ([^{3}H]NMS alone) or 8 ([^{3}H]NMS in the presence of agonist).

G-proteins. Oxotremorine (Figure 10), unlike all other agonists, had no effect on [^{3}H]GDP equilibrium binding to $G_{q/11}$ (Figure 10, lower panel) G-proteins. The rank order of factors of cooperativity between [^{3}H]GDP and agonist binding varied among G-protein classes and was as follows: furmethide = carbachol = oxotremorine > pilocarpine at $G_{i/o}$, carbachol = furmethide > oxotremorine > pilocarpine at $G_{s/olf}$, and carbachol > furmethide > pilocarpine > oxotremorine at $G_{q/11}$ (Table 6).

Discussion

Conventional determination of agonist efficacy of G-protein coupled receptors often utilizes measurements of agonist-induced activation of GTPγS binding. We analysed the role of GDP (the second guanine nucleotide that binds to G-proteins) in the process of activation of the M_2 muscarinic acetylcholine receptors and tested whether changes in its binding could serve as a possible measure of agonist efficacy. The muscarinic agonists studied here differ in structure as well as affinity and efficacy to stimulate GTPγS binding via the M_2 muscarinic receptor (Figure 1). Binding studies show that GTPγS decreases the affinity of agonists as reported previously for the majority of, if not all, GPCRs (Wess, 1997). The decrease in agonist affinity is generally interpreted as being due to disintegration of the receptor/G-protein complex and the liberation of the signalling GTPγS-liganded G-protein α-subunit and complex of βγ subunits (Johnston and Siderovski, 2007). In accordance with previous findings (Haga *et al.*, 1986; Florio and Sternweis, 1989; Tota and Schimerlik, 1990; Shiozaki and Haga, 1992) our data demonstrate that at

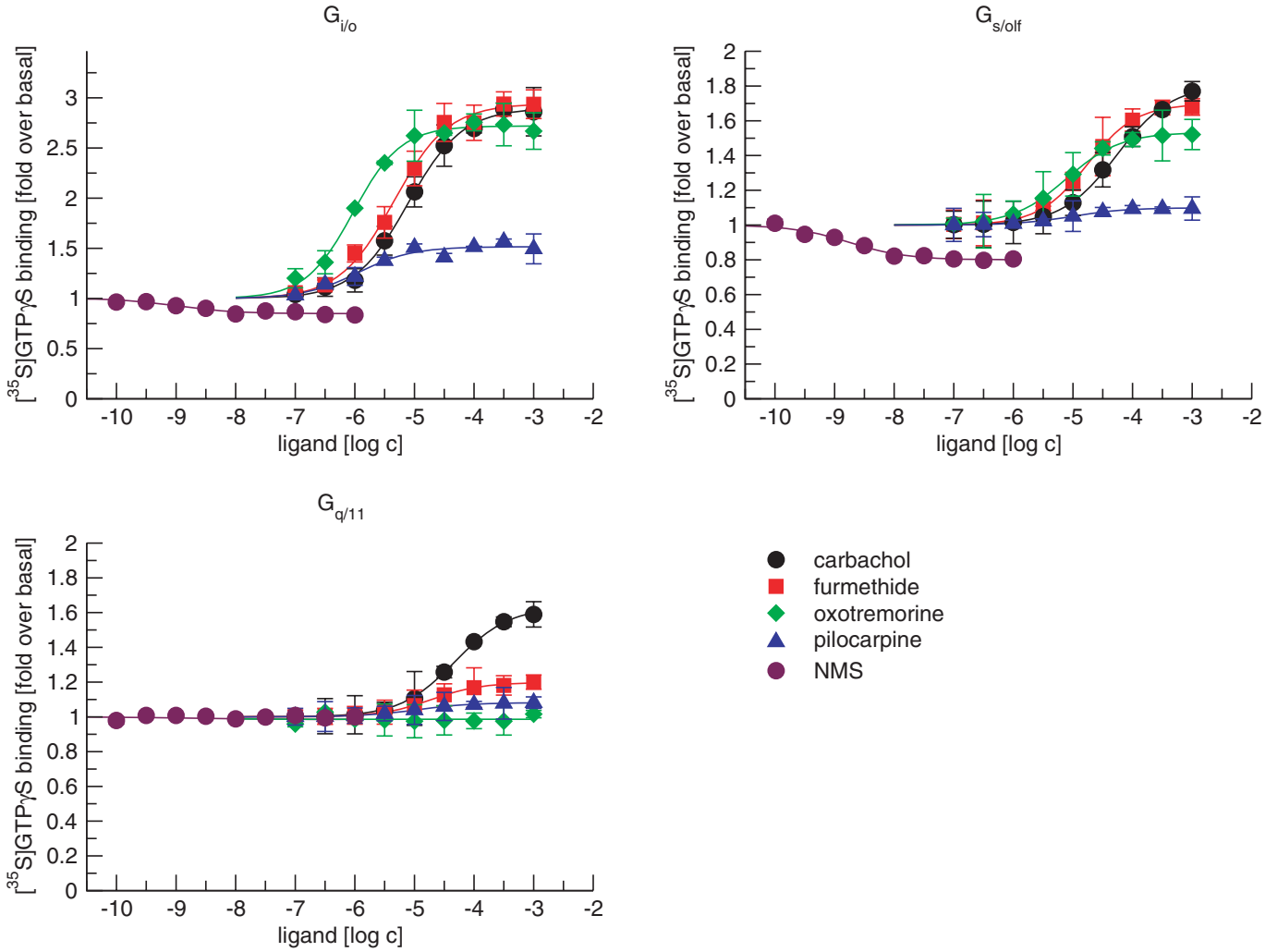

Figure 8

Stimulation of [^{35}S]guanosine-5′-γ–thiotriphosphate (GTPγS) binding to $G_{i/o}$, $G_{s/olf}$ and $G_{q/11}$ G-proteins by agonists. [^{35}S]GTPγS binding to $G_{i/o}$ (upper left), $G_{s/olf}$ (upper right), and $G_{q/11}$ (lower row) G-proteins stimulated by increasing concentrations (abscissa, log M) of agonists carbachol, furmethide oxotremorine and pilocarpine or antagonist N-methylscopolamine (NMS) is expressed as fold over basal (ordinate). Data are presented as mean ± SEM of values from three experiments performed in quadruplicate. Curves were fitted using Equation 2 and results of fits are shown in the Table 4.

the muscarinic M_2 receptors GDP also decreases agonist affinity. In addition, we found that reduction of membrane-bound GDP increases the proportion of high-affinity binding sites for all agonists to a similar extent (Figure 2). Adding GDP back to GDP-less membranes reduces agonist affinity (Figure 7). These findings are consistent with the existence of an agonist low-affinity conformation of the receptor that is complexed with GDP-liganded G-protein, in addition to the agonist low-affinity conformation of receptor that is uncoupled from G-protein upon binding of GTP (Abdulaev *et al.*, 2006).

Although the affinity of agonists at the low-affinity binding state is similar in the presence of either GDP or GTPγS, kinetics of guanine nucleotides binding provide evidence that the molecular mechanisms of modulation of agonist affinity is different. The ability of carbachol to accelerate dissociation and decelerate association of GDP (Figure 4) proves the existence of allosteric interaction between agonist and GDP on the receptor/G-protein complex. On the other hand, the inability of agonists to change the kinetics of GTPγS binding in the absence of GDP (Figure 3, left column; Table 3) is in concert with data obtained in a reconstituted system (Florio and Sternweis, 1989) and the commonly accepted concept that the GTPγS-liganded Gα subunit dissociates from receptor (Johnston and Siderovski, 2007) and therefore the kinetics of GTPγS binding cannot be allosterically regulated by agonists. Receptor-mediated acceleration of GTPγS association in the presence of GDP (Figure 3, upper row; Table 3) is a consequence of accelerated GDP dissociation, while in the absence of GDP the speed of GTPγS binding (irrespective of presence or absence of agonist) is already maximal. Lack of effect of agonists on the rate of GTPγS dissociation in both the presence and absence of GDP (Figure 3, lower row; Table 3) further supports the

Table 5

Effects of carbachol on the kinetics of [^{3}H]GDP binding to $G_{i/o}$ and $G_{s/olf}$ G-proteins

		Control	10 μM carbachol	100 μM carbachol
$G_{i/o}$	k_{obs1} [min^{-1}]	0.055 ± 0.003	0.0056 ± 0.0003**	0.0044 ± 0.0002**
	B_{eq1} [fmol·μg^{-1} protein]	2.1 ± 0.2	1.7 ± 0.2**	0.35 ± 0.03**
	k_{obs2} [min^{-1}]	0.011 ± 0.006		
	B_{eq2} [fmol·μg^{-1} protein]	1.1 ± 0.1		
	k_{off1} [min^{-1}]	0.35 ± 0.03	2.2 ± 0.2**	2.8 ± 0.3**
	k_{off2} [min^{-1}]	0.040 ± 0.004	0.26 ± 0.03**	0.32 ± 0.03**
	f_2 [%]	37 ± 5	38 ± 4	36 ± 5
$G_{s/olf}$	k_{obs} [min^{-1}]	0.031 ± 0.003	0.030 ± 0.003	0.031 ± 0.003
	B_{eq} [fmol·μg^{-1} protein]	0.81 ± 0.04	0.43 ± 0.02**	0.10 ± 0.01**
	k_{off} [min^{-1}]	0.067 ± 0.007	0.12 ± 0.01**	0.20 ± 0.02**

Association rate constants (k_{obs}), equilibrium binding (B_{eq}), dissociation rate constants (k_{off}) and percentages (f_2) of populations were obtained by fitting Equations 6a and 6b or 7a and 7b as appropriate to data from individual experiments shown in Figure 9. Values from better fits are shown. Data are means ± SEM of values from three independent experiments performed in triplicates. **$P < 0.01$, significantly different from control in the absence of carbachol by *t*-test.
GDP, guanosine diphosphate.

Table 6

Parameters of [^{3}H]GDP binding to $G_{i/o}$, $G_{s/olf}$ and $G_{q/11}$ subtypes of G-proteins

	$G_{i/o}$ pK_A	pα	$G_{s/olf}$ pK_A	pα	$G_{q/11}$ pK_A	pα
Carbachol	6.90 ± 0.06	–2.3 ± 0.2	6.87 ± 0.06	–1.2 ± 0.1	6.87 ± 0.02	–0.85 ± 0.09
Furmethide	7.13 ± 0.05	–2.4 ± 0.2	7.10 ± 0.05	–1.0 ± 0.1	7.17 ± 0.06	–0.32 ± 0.05
Oxotremorine	7.93 ± 0.05	–2.1 ± 0.2	7.97 ± 0.05	–0.78 ± 0.08	n.c.	n.c.
Pilocarpine	7.23 ± 0.06	–0.94 ± 0.08	7.19 ± 0.07	–0.24 ± 0.04	7.25 ± 0.08	–0.16 ± 0.03

Equilibrium dissociation constants (K_A) of agonists and factors of cooperativity (α) between agonists and [^{3}H]]GDP binding are expressed as negative logarithms. Constants were obtained by fitting Equation 7 to data from individual experiments shown in Figure 10. Data are means ± SEM of values from three independent experiments performed in quadruplicates.
GDP, guanosine diphosphate.

notion that, under our experimental conditions, the Gα subunit with bound GTPγS is not in physical contact with the receptor.

Agonist-induced allosteric acceleration of GDP dissociation from the Gα subunit strongly implies involvement of this mechanism in regulating the strength (efficacy) of agonist signal transmission to intracellular second messenger pathways. Despite multiple lines of evidence for allosteric interaction between agonist and GDP on receptor-G-protein complex the magnitude of these allosteric interactions has not been quantified so far. Our present data show that the magnitude of negative cooperativity between the four tested agonists displaying different potencies and efficacies, and GDP binding (Figure 6) demonstrate that full agonists (carbachol, furmethide) display significantly stronger negative cooperativity than partial agonists (oxotremorine, pilocarpine). The magnitude of negative cooperativity correlates with agonist efficacy in stimulating GTPγS binding to membranes (furmethide ≥ carbachol > oxotremorine > pilocarpine) (Figure 11). Interestingly, 30 years ago Birdsall *et al*. (1978) showed that agonist efficacy correlates with the ratio of agonist high- and low-affinity binding. Our results confirm these observations and provide a plausible interpretation. Agonist high-affinity binding takes place at a receptor-G-protein complex free of GDP and low-affinity binding occurs at a complex with GDP-liganded G-protein that is low due to negative cooperativity in binding of agonist and GDP. The stronger the negative cooperativity (more negative pα in our experiments) is, the higher the agonist efficacy and the lower the agonist affinity is in the low-affinity binding state. Thus, agonist efficacy correlates with the difference in affinities of the agonist high and low-affinity binding states.

In addition to inhibition of adenylyl cyclase (G_i-mediated), activation of non-preferential G-proteins is associated with strong stimulation of adenylyl cyclase and

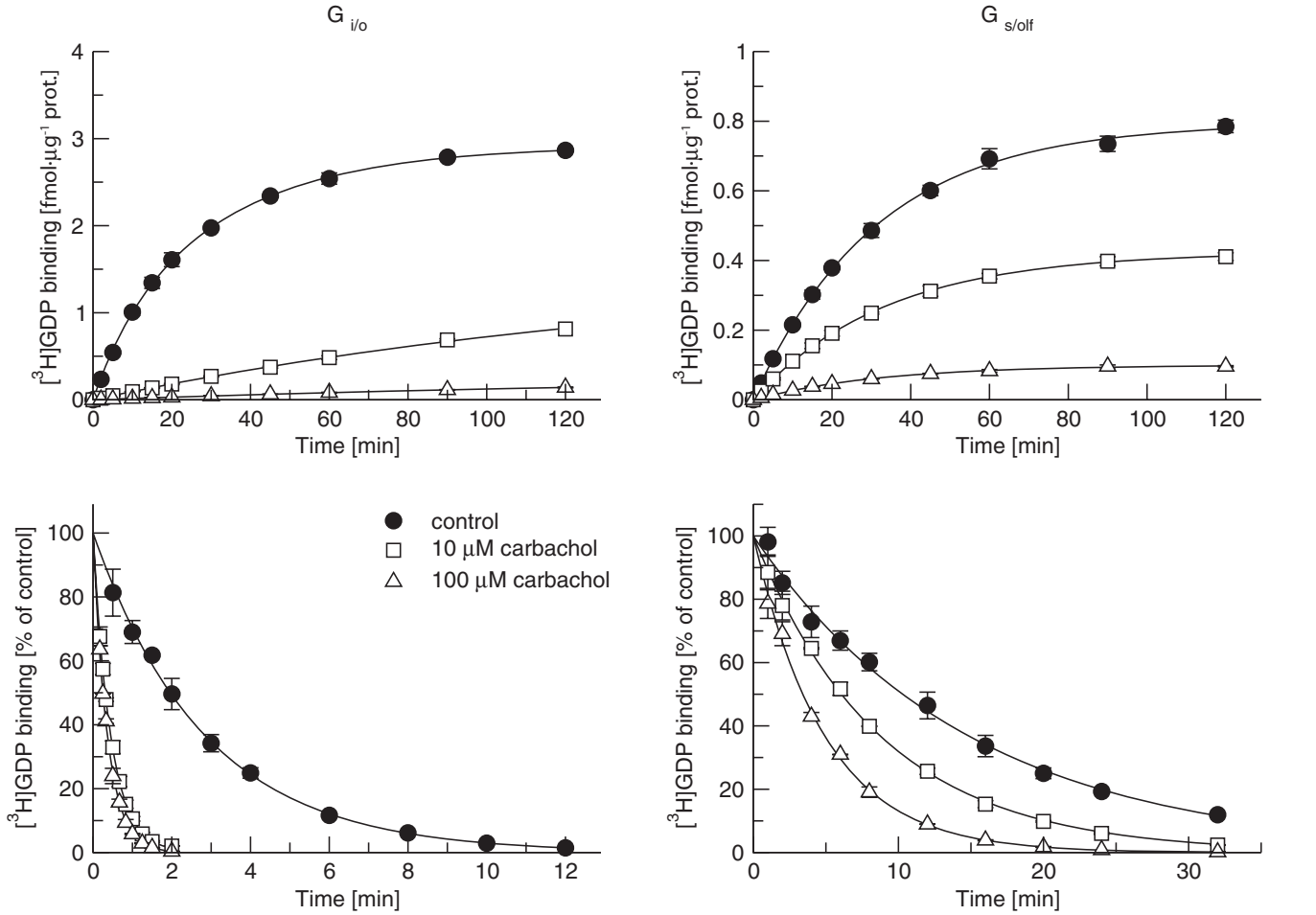

Figure 9

Kinetics of [^{3}H]GDP binding to $G_{i/o}$ and $G_{s/olf}$ G-proteins. Association of 500 nM [^{3}H]GDP with $G_{i/o}$ (top left) and $G_{s/olf}$ (top right) and dissociation of 500 nM [^{3}H]GDP from $G_{i/o}$ (bottom left) and $G_{s/olf}$ (bottom right) subclasses of G-proteins was measured by scintillation proximity assay as described in Methods. GDP-less membranes were pre-incubated for 20 min with either buffer or 10 µM or 100 µM carbachol. Then, 500 nM [^{3}H]GDP was added and association terminated by filtration at the indicated times (abscissa, min). [^{3}H]GDP binding (ordinate) is expressed as fmol per µg of protein. In dissociation measurements, GDP-less membranes were equilibrated for two hours in the presence of 500 nM [^{3}H]GDP. Dissociation was then initiated by the addition of 50 µM GDP alone or in combination with carbachol at 10 µM or 100 µM and terminated at indicated times (abscissa, min). [^{3}H]GDP binding (ordinate) is expressed as per cent of binding at the beginning of dissociation. Data are expressed as mean ± SEM of values from three experiments performed in triplicate. Curves were fitted using Equations 5a and 5b (association) or 6a and 6b (dissociation). Results of fits are shown in Table 5.

relatively weak effects on accumulation of inositol phosphates (G_q-medited) by muscarinic M_2 receptors was observed repeatedly (Ashkenazi *et al.*, 1987; Burford *et al.*, 1995; Jakubík *et al.*, 1996; Michal *et al.*, 2001; 2007). In SPAs, furmethide, carbachol and pilocarpine stimulated GTPγS binding to preferential $G_{i/o}$ as well as non-preferential $G_{s/olf}$ and $G_{q/11}$ G-proteins. In contrast, oxotremorine stimulated GTPγS binding only to $G_{i/o}$ and $G_{s/olf}$ G-proteins (Figure 8, Table 4). Different orders of efficacies at individual G-protein classes can be explained by the concept of agonist specific conformations (Kenakin, 2003), where individual agonists induce different receptor conformations that differ in the ability to activate individual classes of G-proteins.

In agreement with an allosteric mode of action, affinities of GDP for the Gα subunits calculated from interactions with all of the tested agonists are the same (between 2.9 and 3.4 µM; Figures 6, 7 and 10) and correspond well to published values (Thomas *et al.*, 1993) as well as results of [^{3}H]GDP kinetics (Figures 4 and 9; Tables 3 and 5) and [^{3}H]GDP saturation binding (Figure 5). Thus, changes in GDP affinity or kinetics are good measures of agonist efficacy at the $G_{i/o}$-coupled M_2 muscarinic receptor. In practice, being the first step next to receptor activation, [^{3}H]GDP binding appears to be a more direct measure of receptor activation than GTPγS binding or second messenger levels in case of M_2 receptors, and this may be so at other $G_{i/o}$ coupled GPCRs. However, this assay requires laborious preparation of membranes free of GDP. Agonist induced changes in GTPγS binding were demonstrated in fused $G_s\alpha/\beta_2$-adrenoceptors where agonist efficacy was well reflected by changes in the kinetics of GTPγS binding (Wenzel-Seifert and Seifert, 2000; Seifert *et al.*, 2001).

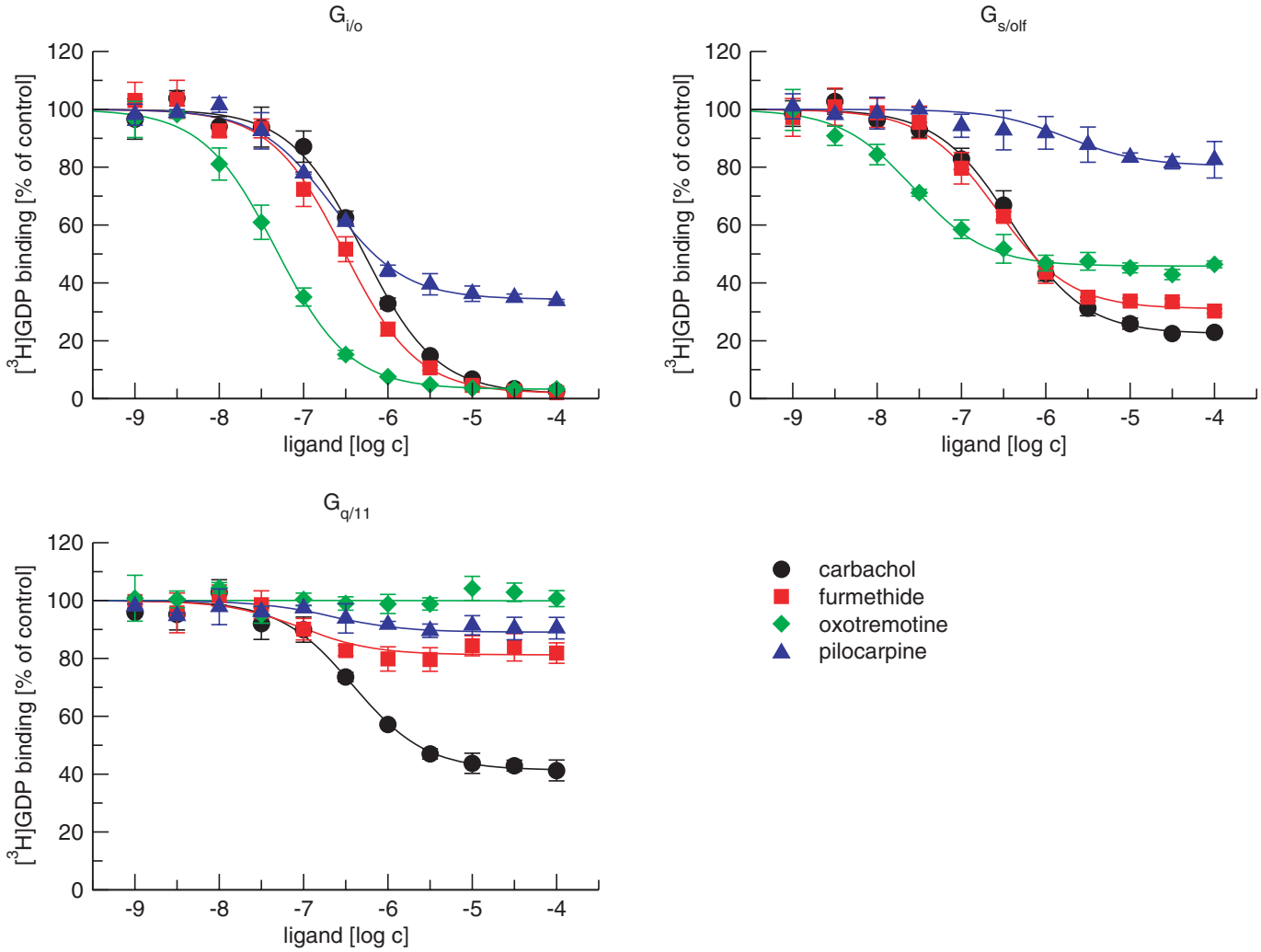

Figure 10

Allosteric interactions between agonists and [^{3}H]GDP at individual G-proteins. The magnitude of allosteric interactions between agonists (carbachol, furmethide, oxotremorine, pilocarpine) and [^{3}H]GDP was measured directly as changes in equilibrium binding of 10 μM [^{3}H]GDP to $G_{i/o}$ (upper left), $G_{s/olf}$ (upper right) or $G_{q/11}$ (lower row) G-proteins in the presence of increasing ligand concentration (abscissa, log M) via scintillation proximity assay as described in Methods. Data are presented as mean ± SEM of values from three experiments performed in quadruplicate. Curves were fitted using Equation 7. Results of fits are shown in the Table 6.

However, in concert with the involvement of agonist-induced decrease in GDP affinity in G-protein activation, GDP differentially and concentration-dependently influenced relative efficacies of partial agonists in increasing GTPγS binding (Wenzel-Seifert and Seifert, 2000). In accordance with previous findings (Florio and Sternweis, 1989), agonists at M_2 receptors under our experimental conditions do not change the kinetics of GTPγS binding in the absence of GDP (Figure 3). Thus, while a change in the kinetic of GTPγS binding is a good measure of activation of physically coupled G-protein/β_2- adrenoceptors, kinetics of GDP binding seem to be a closer measure in case of M_2 muscarinic receptors and likely in other GPCR. Another drawback of GTPγS binding measurements is their dependence on the concentration of GDP that strongly affects outcome of the experiments (Figure 3). Also, unlike GDP binding, GTPγS concentration–response curve has to be measured under non-equilibrium conditions (Figure 3).

The data presented here show some interesting aspects of the process of receptor activation. NMS was reported as an inverse agonist at the M_2 receptor (Jakubík *et al.*, 1995; Burstein *et al.*, 1997) and behaved as inverse agonist under our experimental conditions (Figures 1 and 8). Although positive cooperativity in binding with GDP would be expected, our data show that the cooperativity between NMS and GDP is neutral (Figures 6 and 7) and NMS only slightly slows down GDP dissociation (Figure 4 right), implying different mechanisms underlying the inverse agonist nature of NMS. One possible explanation may be that NMS stabilizes the receptor in the ground state (inactive conformation) (Hulme *et al.*, 2003) that leads to reduction of spontaneous transition of the ligand-free receptor to an active state and slower rate of GDP

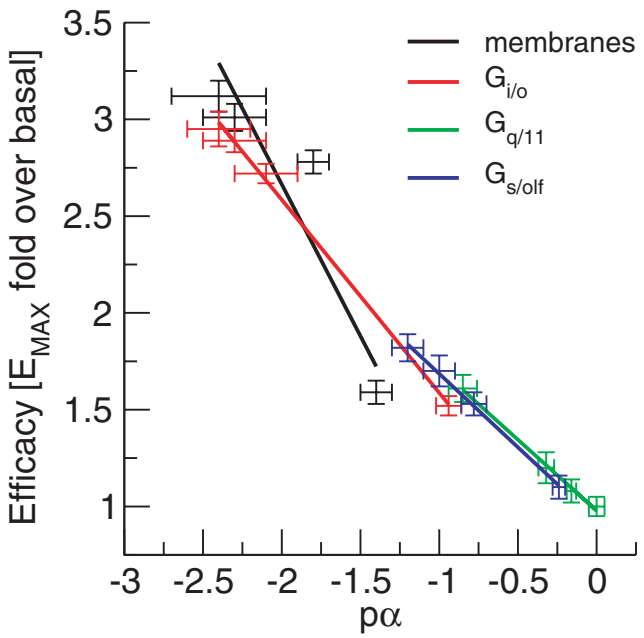

Figure 11

Correlation of binding cooperativity between agonist and GDP with maximal stimulation of [^{35}S]guanosine-5′-γ–thiotriphosphate (GTPγS) binding by agonist. Values of maximum of [^{35}S]GTPγS binding (E_{MAX}) to membranes, $G_{i/o}$, $G_{s/olf}$ and $G_{q/11}$ (Tables 1 and 4) are plotted against the negative logarithms of the factor of binding cooperativity between agonist and GDP (pα) (results of Figure 6 and Table 6). Lines: 2D (Deming) linear regression of the data.

dissociation. Significantly, this difference in mechanisms of agonism and inverse agonism cannot be revealed by measurement of GTPγS binding.

The second interesting aspect of our study is derived from data shown in Figure 9 that illustrates that carbachol slows down association of GDP with $G_{i/o}$ G-proteins but does not change the rate of association of GDP with $G_{s/olf}$ G-proteins. These data suggest that interaction of the M_2 receptor with preferential $G_{i/o}$ G-proteins differs from that with non-preferential $G_{s/olf}$ G-proteins. One possible explanation is that $G_{i/o}$ G-proteins precouple to M_2 receptors while $G_{s/olf}$ do not (Shea and Linderman, 1997; Hein *et al.*, 2005), where precoupling gives an agonist a chance to influence GDP association while collision coupling does not. However, demonstration of this difference in coupling requires further detailed analysis. Again, this difference in kinetics at $G_{i/o}$ and $G_{s/olf}$ classes of G-proteins cannot be revealed by measurement of GTPγS binding.

In conclusion, we have demonstrated that the negative cooperativity between GDP and agonist binding played a key role in signal transduction via the M_2 receptor. Agonist-induced low-affinity conformation of the Gα G-protein subunit for GDP leads to accelerated dissociation of bound GDP that in turn accelerates binding of GTP and G-protein activation. Thus, stronger negative cooperativity between a given agonist and GDP binding leads to a bigger shift of the GDP/GTP affinity ratio resulting in a higher rate of GTP binding and agonist efficacy. Our data demonstrated benefits of GDP binding measurements that can reveal mechanistic differences that are not apparent in measurements of GTP binding, as was demonstrated in case of inverse agonists versus agonists or $G_{i/o}$ versus $G_{s/olf}$ G-proteins. Measurements of GDP binding therefore provide additional information beyond that obtained from GTP binding measurements.

Acknowledgements

This work was supported by Project AV0Z 50110509, the grants of the Grant Agency of the Czech Republic 305/09/0681, the Grant Agency of the Czech Academy of Sciences IAA500110703, and the Ministry of Education, Youth and Sports, Czech Republic LC554, and NIH grant NS25743.

Conflicts of interest

None.

References

Abdulaev NG, Ngo T, Ramon E, Brabazon DM, Marino JP, Ridge KD (2006). The receptor-bound "empty pocket" state of the heterotrimeric G-protein alpha-subunit is conformationally dynamic. Biochemistry 45: 12986–12997.

Alexander SPH, Mathie A, Peters JA (2009). Guide to receptors and channels (GRAC). 4th edn. Br J Pharmacol 158 (Suppl. 1): S1–S254.

Ashkenazi A, Winslow JW, Peralta EG, Peterson GL, Schimerlik MI, Capon DJ *et al.* (1987). An M2 muscarinic receptor subtype coupled to both adenylyl cyclase and phosphoinositide turnover. Science 238: 672–675.

Birdsall NJ, Burgen AS, Hulme EC (1978). The binding of agonists to brain muscarinic receptors. Mol Pharmacol 14: 723–736.

Burford NT, Tobin AB, Nahorski SR (1995). Differential coupling of m1, m2 and m3 muscarinic receptor subtypes to inositol 1,4,5-trisphosphate and adenosine 3′,5′-cyclic monophosphate accumulation in Chinese hamster ovary cells. J Pharmacol Exp Ther 274: 134–142.

Burstein ES, Spalding TA, Brann MR (1997). Pharmacology of muscarinic receptor subtypes constitutively activated by G proteins. Mol Pharmacol 51: 312–319.

Cheng Y, Prusoff WH (1973). Relationship between the inhibition constant (K1) and the concentration of inhibitor which causes 50 per cent inhibition (I50) of an enzymatic reaction. Biochem Pharmacol 22: 3099–3108.

DeLapp NW, McKinzie JH, Sawyer BD, Vandergriff A, Falcone J, McClure D *et al.* (1999). Determination of [35S]guanosine-5″-O-(3-thio)triphosphate binding mediated by cholinergic muscarinic receptors in membranes from Chinese hamster ovary cells and rat striatum using an anti-G protein scintillation proximity assay. J Pharmacol Exp Ther 289: 946–955.

De Lean A, Stadel JM, Lefkowitz RJ (1980). A ternary complex model explains the agonist-specific binding properties of the adenylate cyclase-coupled beta-adrenergic receptor. J Biol Chem 255: 7108–7117.

Ehlert FJ (1988). Estimation of the affinities of allosteric ligands using radioligand binding and pharmacological null methods. Mol Pharmacol 33: 187–194.

Ferguson KM, Higashijima T, Smigel MD, Gilman AG (1986). The influence of bound GDP on the kinetics of guanine nucleotide binding to G proteins. J Biol Chem 261: 7393–7399.

Florio VA, Sternweis PC (1989). Mechanisms of muscarinic receptor action on Go in reconstituted phospholipid vesicles. J Biol Chem 264: 3909–3915.

Haga K, Haga T, Ichiyama A (1986). Reconstitution of the muscarinic acetylcholine receptor. Guanine nucleotide-sensitive high affinity binding of agonists to purified muscarinic receptors reconstituted with GTP-binding proteins (Gi and Go). J Biol Chem 261: 10133–10140.

Hein P, Frank M, Hoffmann C, Lohse MJ, Bünemann M (2005). Dynamics of receptor/G protein coupling in living cells. EMBO J 24: 4106–4114.

Hulme EC, Lu ZL, Saldanha JW, Bee MS (2003). Structure and activation of muscarinic acetylcholine receptors. Biochem Soc Trans 31: 29–34.

Jakubík J, Bačáková L, el-Fakahany EE, Tuček S (1995). Constitutive activity of the M1-M4 subtypes of muscarinic receptors in transfected CHO cells and of muscarinic receptors in the heart cells revealed by negative antagonists. FEBS Lett 377: 275–279.

Jakubík J, Bačáková L, Lisá V, el-Fakahany EE, Tuček S (1996). Activation of muscarinic acetylcholine receptors via their allosteric binding sites. Proc Natl Acad Sci U S A 93: 8705–8709.

Jakubík J, Bačáková L, El-Fakahany EE, Tuček S (1997). Positive cooperativity of acetylcholine and other agonists with allosteric ligands on muscarinic acetylcholine receptors. Mol Pharmacol 52: 172–179.

Jakubík J, El-Fakahany EE, Doležal V (2006). Differences in kinetics of xanomeline binding and selectivity of activation of G proteins at M(1) and M(2) muscarinic acetylcholine receptors. Mol Pharmacol 70: 656–666.

Johnston CA, Siderovski DP (2007). Receptor-mediated activation of heterotrimeric G-proteins: current structural insights. Mol Pharmacol 72: 219–230.

Kenakin T (2003). Ligand-selective receptor conformations revisited: the promise and the problem. Trends Pharmacol Sci 24: 346–354.

Kent RS, De Lean A, Lefkowitz RJ (1980). A quantitative analysis of beta-adrenergic receptor interactions: resolution of high and low affinity states of the receptor by computer modeling of ligand binding data. Mol Pharmacol 17: 14–23.

Michal P, Lysíková M, Tuček S (2001). Dual effects of muscarinic M(2) acetylcholine receptors on the synthesis of cyclic AMP in CHO cells: dependence on time, receptor density and receptor agonists. Br J Pharmacol 132: 1217–1228.

Michal P, El-Fakahany EE, Doležal V (2007). Muscarinic M2 receptors directly activate Gq/11 and Gs G-proteins. J Pharmacol Exp Ther 320: 607–614.

Oldham WM, Hamm HE (2008). Heterotrimeric G protein activation by G-protein-coupled receptors. Nat Rev Mol Cell Biol 9: 60–71.

Seifert R, Wenzel-Seifert K, Gether U, Kobilka BK (2001). Functional differences between full and partial agonists: evidence for ligand-specific receptor conformations. J Pharmacol Exp Ther 297: 1218–1226.

Shea L, Linderman JJ (1997). Mechanistic model of G-protein signal transduction. Determinants of efficacy and effect of precoupled receptors. Biochem Pharmacol 53: 519–530.

Shiozaki K, Haga T (1992). Effects of magnesium ion on the interaction of atrial muscarinic acetylcholine receptors and GTP-binding regulatory proteins. Biochemistry 31: 10634–10642.

Thomas TC, Schmidt CJ, Neer EJ (1993). G-protein alpha o subunit: mutation of conserved cysteines identifies a subunit contact surface and alters GDP affinity. Proc Natl Acad Sci U S A 90: 10295–10298.

Tota MR, Schimerlik MI (1990). Partial agonist effects on the interaction between the atrial muscarinic receptor and the inhibitory guanine nucleotide-binding protein in a reconstituted system. Mol Pharmacol 37: 996–1004.

Wenzel-Seifert K, Seifert R (2000). Molecular analysis of beta(2)-adrenoceptor coupling to G(s)-, G(i)-, and G(q)-proteins. Mol Pharmacol 58: 954–966.

Wess J (1997). G-protein-coupled receptors: molecular mechanisms involved in receptor activation and selectivity of G-protein recognition. FASEB J 11: 346–354.